AMERICAN SOCIETY FOR MICROBIOLOGY | Infection and Immunity®

BACTERIAL INFECTIONS

Strain-Dependent Effect of Capsule on Transmission and Persistence in an Infant Mouse Model of Group A *Streptococcus* Infection

Luis Alberto Vega,[a] Misu A. Sanson,[a] Brittany J. Shah,[a] Anthony R. Flores[a,b]

[a]Division of Infectious Diseases, Department of Pediatrics, McGovern Medical School, University of Texas Health Sciences Center at Houston, Houston, Texas, USA
[b]Center for Antimicrobial Resistance and Microbial Genomics, University of Texas Health Sciences Center at Houston, Houston, Texas, USA

ABSTRACT *Streptococcus pyogenes* (group A *Streptococcus* [GAS]) is a human pathogen responsible for a wide range of diseases. Asymptomatic carriage of GAS in the human pharynx is commonplace and a potential reservoir for GAS transmission. Early studies showed that GAS transmission correlated with high bacterial burdens during the acute symptomatic phase of the disease. Human studies and the nonhuman primate model are generally impractical for investigation of the bacterial mechanisms contributing to GAS transmission and persistence. To address this gap, we adapted an infant mouse model of pneumococcal colonization and transmission to investigate factors that influence GAS transmission and persistence. The model recapitulated the direct correlation between GAS burden and transmission during the acute phase of infection observed in humans and nonhuman primates. Furthermore, our results indicate that the ratio of colonized to uncolonized hosts influences the rates of GAS transmission and persistence. We used the model to test the hypothesis that capsule production influences GAS transmission and persistence in a strain-dependent manner. We detected significant differences in rates of transmission and persistence between capsule-positive (*emm3*) and capsule-negative (*emm87*) GAS strains. Capsule was associated with higher levels of GAS shedding, independent of the strain background. In contrast to the capsule-positive *emm3* strain, restoring capsule production in *emm87* GAS did not increase transmissibility, and the absence of capsule enhanced persistence only in the capsule-negative (*emm87*) strain background. These data suggest that strain background (capsule positive versus capsule negative) influences the effect of capsule in GAS transmission and persistence and that as-yet-undefined factors are required for the transmission of capsule-negative *emm* types.

KEYWORDS group A *Streptococcus*, mouse, nasopharyngeal colonization, persistence, transmission, capsule

Streptococcus pyogenes (group A *Streptococcus* [GAS]) is an exclusively human pathogen that primarily colonizes the epithelia of the throat and skin. Several clinically important invasive GAS serotypes are responsible for an upsurge in diseases associated with high mortality rates over the past 30 years (1). Efforts to reduce the incidence of worldwide GAS-related disease via a vaccine that prevents GAS colonization and transmission have thus far met with little success (2, 3). Therefore, it is critical to better understand the mechanisms of GAS colonization, transmission, and persistence to develop alternative strategies to mitigate the impact of GAS disease.

In addition to disease, GAS is commonly carried in the human throat in the absence of symptoms. Asymptomatic colonization (asymptomatic carriage or carriage) is defined as the presence of GAS in the throat in the absence of acute symptoms (4). In one

Citation Vega LA, Sanson MA, Shah BJ, Flores AR. 2020. Strain-dependent effect of capsule on transmission and persistence in an infant mouse model of group A *Streptococcus* infection. Infect Immun 88:e00709-19. https://doi.org/10.1128/IAI.00709-19.

Editor Nancy E. Freitag, University of Illinois at Chicago

Address correspondence to Anthony R. Flores, anthony.r.flores@uth.tmc.edu.

Received 10 September 2019
Returned for modification 20 October 2019
Accepted 15 January 2020
Accepted manuscript posted online 3 February 2020
Published 23 March 2020

of the only longitudinal GAS carriage studies in children, over a 4-year study period, >50% of pediatric subjects were classified as carriers (5), indicating that asymptomatic carriers are commonplace and a reservoir for potential GAS transmission. GAS is spread primarily by direct person-to-person transmission, through the inhalation of respiratory droplets, or through skin contact (6). In studies of patients with a high incidence of GAS respiratory tract infection, Hamburger et al. showed that GAS transmission correlated with high titers of streptococcal output (i.e., shedding) (7, 8). Furthermore, those studies also indicated that shedding of streptococci by infected individuals occurs primarily in the early stages of disease, when the bacterial burden is highest (7). Not all individuals that were "strongly positive" for colonization with streptococci transmitted GAS (8), suggesting that the relationship between carriage, disease, and transmission is complex and likely dependent upon host and pathogen factors.

Substantial gaps in knowledge exist regarding the host and pathogen mechanisms (e.g., GAS virulence factor expression, host inflammation, and superinfection) that promote shedding from infected individuals and result in GAS transmission. Patient studies to identify the immune responses that distinguish GAS carriage from pharyngitis in children have been inconclusive (9). The diversity of circulating strains, the complexity of individual adaptive immunity, and the need for sequential sampling to accurately define infection (10) preclude large-scale studies to identify factors influencing GAS transmission from carriers. Therefore, animal models are needed to investigate the mechanisms of GAS carriage and transmission.

Several animal models exist to investigate the mechanisms of GAS colonization and disease (11–13), but few examine transmission (14, 15). The nonhuman primate model accurately reproduces GAS pharyngitis (16) but is impractical for the study of transmission and persistence. Recently, Zafar et al. used infant mice as a model of *Streptococcus pneumoniae* nasal colonization and transmission (17) to show that pneumococcal shedding correlates directly with transmission rates and is influenced by colonization density. These results are reminiscent of the observations by Hamburger et al., making it a promising model to dissect the mechanisms of GAS transmission. In a follow-up study, Zafar et al. showed that the production of polysaccharide capsule enhanced pneumococcal shedding and was required for the transmission of *S. pneumoniae* (18). In GAS, the nonimmunogenic hyaluronic acid (HA) capsule is associated with enhanced resistance to immune clearance by phagocytic cells and increased virulence (19–21). Acapsular mutants of capsule-positive strains have a diminished capacity for throat colonization in murine and nonhuman primate models (11, 22). In contrast, several studies have linked the absence of capsule to enhanced GAS adherence and internalization into epithelial cells (23–25) as well as increased persistence during asymptomatic carriage in humans and animal models (26–28). The recent emergence of capsule-negative GAS *emm* types (e.g., *emm4*, *emm22*, *emm28*, *emm87*, and *emm89*) (29–32) suggests that such strains have developed strategies for transmission and persistence in an *emm* type-dependent manner in the absence of capsule.

In this study, we adapted the infant mouse model for the study of GAS transmission and persistence to test the hypothesis that capsule production significantly influences GAS transmission and persistence in a strain-dependent manner. We demonstrate that our model recapitulates the association of bacterial burden with shedding and transmission observed in humans and nonhuman primate models. Our data suggest that capsule production (or a lack thereof) has driven the selection of contrasting infectious strategies among GAS serotypes. Our experimentation establishes the infant mouse model of intranasal colonization as a useful tool for studies examining mechanisms of GAS transmission and carriage.

RESULTS

Shedding and persistence of *emm3* serotype GAS in infant CD-1 mice are inoculum dependent. To establish the infant mouse model of GAS transmission and carriage, we first determined a dose response to GAS infection of infant CD-1 mice and assessed titers of shed streptococci. We initiated studies in the CD-1 mouse background

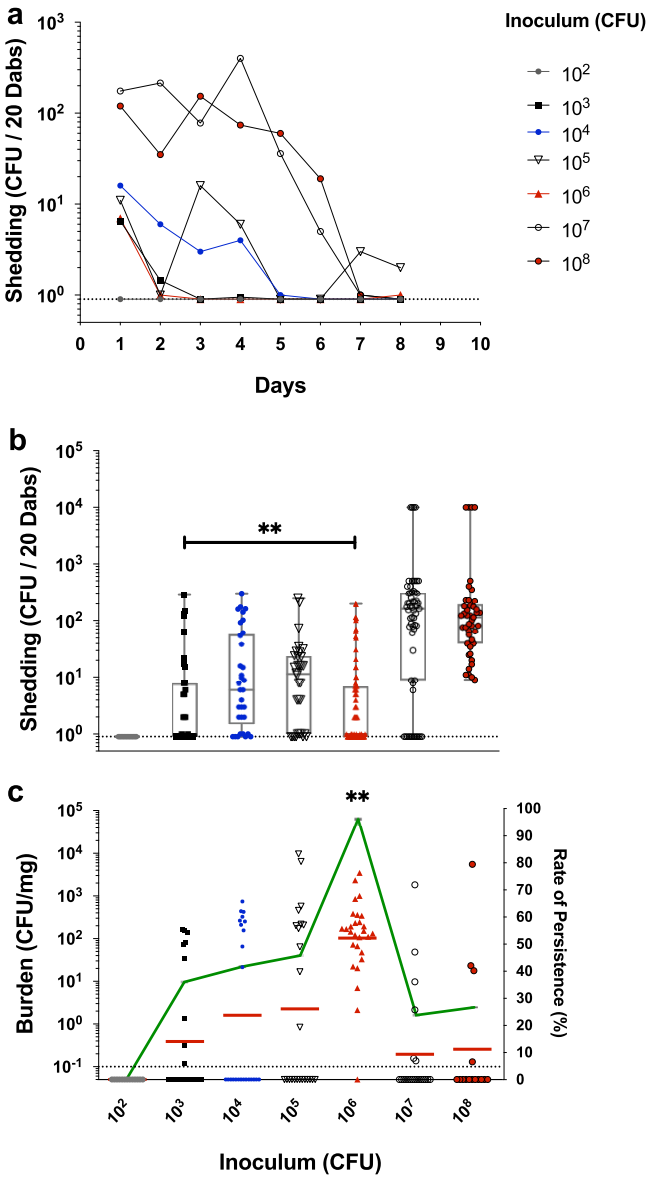

FIG 1 Shedding and persistence of *emm3* serotype GAS in infant CD-1 mice are inoculum dependent. (a and b) Shedding titers (CFU) of MGAS10870 from inoculated infant mice in CD-1 litters were enumerated daily over the period of days 1 to 9 postinoculation, and the median shed titers were detected throughout this period (a) and during the acute shedding phase of infection (days 1 to 3 postinoculation) (b). (c) Intranasal MGAS10870 tissue burden (left axis) and rate of persistence (right axis) in CD-1 litters were assessed at day 11 postinoculation and quantified as streptococcal CFU per milligram of homogenized nasal tissue. The medians and ranges of detected titers (box-and-whisker plot) are shown to indicate the median shedding titer and rate (a and b). The geometric mean GAS burdens (red lines) are shown to indicate the mean colonization burden and persistence rate (green line) (c). Litters are indicated by the inocula (CFU) administered, shown on the *x* axis. The limit of detection is indicated by the dotted line (shedding titer, 1 CFU; colonization burden, 0.1 CFU/mg). Significance was determined by a Mann-Whitney U test (**, $P < 0.01$).

given the extensive experimental data, including colonization (33, 34). A range of inocula of the *emm3* serotype MGAS10870 strain was administered intranasally to 4-day-old CD-1 pups, and shedding of GAS was monitored daily. The highest titers of shed MGAS10870 across all inocula were detected in the 3 days after inoculation (Fig. 1a). Significantly higher median shedding titers were consistently detected from mice inoculated with $\geq 10^7$ CFU over this period ($P < 0.01$) (Fig. 1b). No shed GAS bacteria were detected from mice inoculated with 10^2 CFU (Fig. 1a and b). Following this acute

TABLE 1 Summary of GAS transmission dynamics in infant mice

Strain	Ratio[a]	Inoculum (CFU)[b]	No. of litters	No. of index mice	No. of contact mice	% transmission[c]	Transmission comparison(s) (ratio-CFU)[d]
emm3	1:1	10^4	3	20	20	0	
		10^6	3	20	20	0	
		10^7	3	22	21	19.1	1:1-10^4, 10^6*
	1:2	10^4	3	13	28	0	
		10^6	3	12	23	47.8	1:1-10^6***
							1:2-10^4#
		10^7	3	11	22	90.9	1:1-10^7#
							1:2-10^6**
emm3$^{\Delta hasA}$	1:1	10^7	3	12	14	0	*emm3*, 1:1-10^7 ($P = 0.07$)
emm87	1:1	10^4	2	11	11	27.3	*emm3*, 1:1-10^4*
		10^7	2	12	13	53.8	emm3, 1:1-10^7 ($P = 0.13$)
	1:2	10^4	2	9	16	0	
		10^7	3	10	18	38.9	*emm3*, 1:2-10^7***
emm87(*hasA*^{emm3})	1:1	10^7	2	13	14	14.3	*emm87*, 1:1-10^7*
emm87(*hasA*^{emm3}-Δ*covS*)	1:1	10^7	3	18	18	5.6	*emm87*, 1:1-10^7**
emm87$^{\Delta covS}$	1:1	10^7	2	13	14	0	*emm87*, 1:1-10^7**

[a]Index-to-contact ratio of infant mice in litters.
[b]CFU administered to index mice.
[c]Transmission rate expressed as a percentage of contact mice with a detectable intranasal burden of the corresponding GAS strain.
[d]Comparison of transmission rates using Fisher's exact test (two tailed) (*, $P < 0.05$; **, $P < 0.01$; ***, $P < 0.001$; #, $P < 0.0001$).

shedding phase of colonization, shed MGAS10870 bacteria were detected mostly from infant mice administered the highest inocula (Fig. 1a).

The nasal tissues of inoculated infant mice were harvested at 2 weeks of age (day 11 postinoculation) to measure the persistence of GAS intranasal colonization. The maximum rate of persistence (96%) was observed in litters inoculated with 10^6 CFU of MGAS10870, in which a mean GAS burden of 10^2 CFU/mg of homogenized nasal tissue was detected (Fig. 1c). The burden of MGAS10870 in colonized infant mice at day 11 postinoculation ranged predominantly between 10 and 10^3 CFU/mg of homogenized nasal tissue. No morbidity resulted from inoculation with MGAS10870, and weight gain in infant mice differed only from that of control litters inoculated with sterile phosphate-buffered saline (PBS) in litters administered 10^8 CFU (see Fig. S1 in the supplemental material). Persistent GAS colonization of nasal tissues in infant mice consisted of a low burden ($\sim 10^2$ CFU/mg) of colonizing streptococci, and an ~50% carriage rate was achieved with an inoculum of as few as 10^4 CFU (Fig. 1c). Thus, the data demonstrate that GAS shedding and persistence in the infant mouse nasal cavity are experimentally feasible and inoculum dependent.

Transmission of *emm3* serotype GAS in infant CD-1 mice is associated with high shedding titers and influenced by the index-to-contact ratio. To investigate the relationships between inoculum size, GAS burden, and shedding titer and the transmission of MGAS10870 across CD-1 littermates, we next examined differing ratios of inoculated (index) to uninfected (contact) infant mice in experimental litters. Index mice were administered GAS inocula (10^4, 10^6, and 10^7 CFU) shown to produce detectable shedding and persistence (Fig. 1). GAS transmission was monitored by the detection of both shedding titers (up to day 9 postinoculation) and the intranasal burden of MAGS10870 harvested from contact mice (days 3 and 11).

The detected shedding titers and GAS burdens revealed that the rates of GAS transmission differed between 1:1 and 1:2 index-to-contact ratio litters (Table 1; Fig. 2 and 3). The highest titers of shed MGAS10870 were detected from index mice in the 3 days immediately following inoculation (Fig. 2a to d). The numbers of shed streptococci were directly proportional to the inoculum administered to index mice (Fig. 2a and b). The median shedding titer detected from index mice inoculated with 10^7 CFU was significantly higher than those in the other inoculated mice during this acute shedding phase (days 1 to 3; $P < 0.05$). Most shedding of GAS from contact mice was

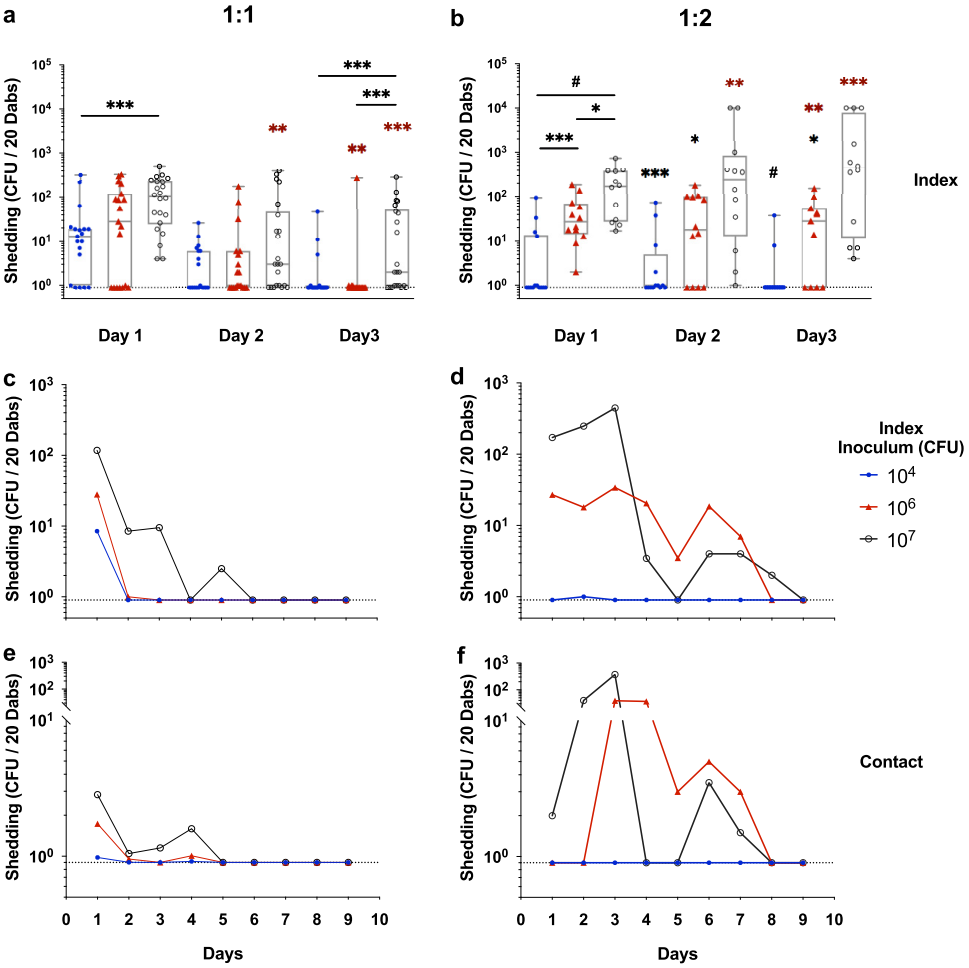

FIG 2 Shedding of *emm3* serotype GAS in infant CD-1 mice is inoculum dependent and influenced by the index-to-contact ratio. (a and b) Shedding titers of MGAS10870 from index mice in CD-1 litters inoculated at 1:1 (a) and 1:2 (b) index-to-contact ratios were detected during the acute shedding phase (days 1 to 3 postinoculation). (c and d) Shedding titers (CFU) of MGAS10870 from index mice in CD-1 litters inoculated at 1:1 (c) and 1:2 (d) index-to-contact ratios were detected throughout the monitoring period (days 1 to 9 postinoculation). (e and f) Shedding titers of MGAS10870 from contact mice in the same such litters were likewise assessed. The median shed titers, detected daily, are shown. Litters are indicated by the inocula (CFU) administered in the key adjacent to the graphs, and days postinoculation are enumerated on the *x* axis. The limit of detection is indicated by a dotted line (shedding titer, 1 CFU). Statistically significant differences in median shed titers were determined between inocula (black) and between index-to-contact ratios (red) by a Mann-Whitney U test (*, $P < 0.05$; **, $P < 0.01$; ***, $P < 0.001$; #, $P < 0.0001$).

detected in litters that had been administered high inocula ($\geq 10^6$ CFU) (Fig. 2e and f). Inoculum-dependent differences in detected shedding titers were greatest at an index-to-contact ratio of 1:2 (Fig. 2b, d, and f). Shed GAS bacteria were detected at a significantly higher frequency and titer in the 1:2 index-to-contact ratio litters administered the highest inocula ($\geq 10^6$ CFU) (Fig. 2b and d).

The intranasal burden of MGAS10870 measured in randomly selected contact and index mice at day 3 postinoculation revealed a low GAS transmission rate in litters inoculated at a 1:1 index-to-contact ratio, despite a detectable GAS burden in all but two selected index mice (Table 1; Fig. 3a). The MGAS10870 burden in litters inoculated at a 1:2 index-to-contact ratio further indicated that the GAS transmission rate was directly proportional to the inoculum administered to index littermates (Table 1; Fig. 3b). Additionally, shedding titers detected at day 3 postinoculation corresponded with bacterial burdens (Fig. 2b and d; Fig. 3b). The MGAS10870 burden across index mice ranged from 1 to 10^3 CFU/mg of homogenized nasal tissue, and inoculum-dependent differences in burdens were more evident in the 1:2 index-to-contact ratio litters,

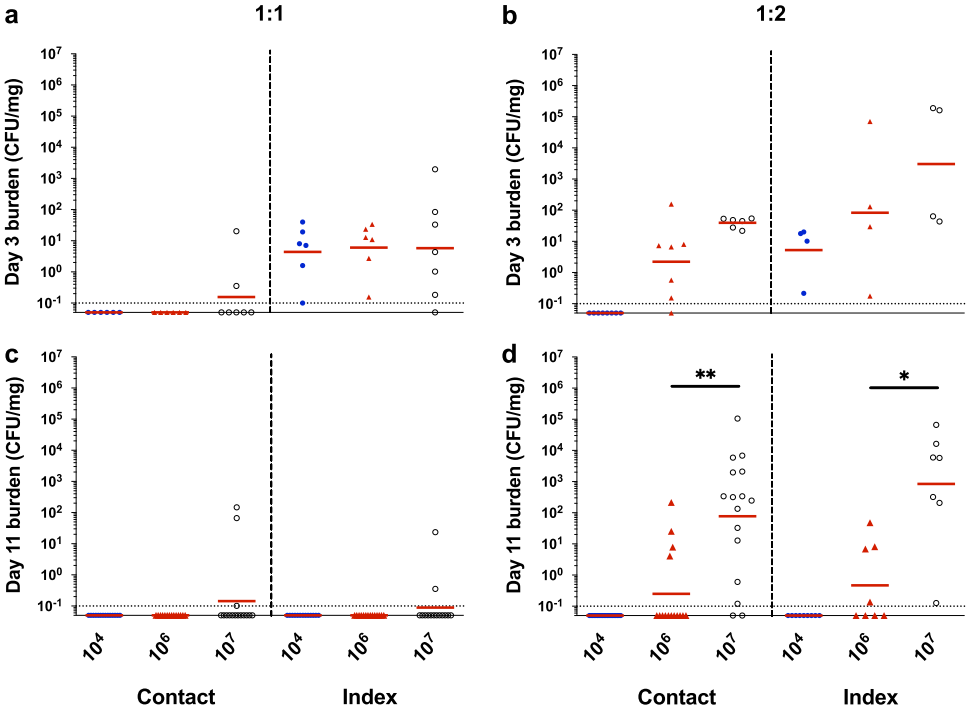

FIG 3 Transmission of *emm3* serotype GAS in infant CD-1 mice is influenced by the index-to-contact ratio. (a and b) Intranasal MGAS10870 tissue burdens in randomly selected contact and index mice in 1:1 (a) and 1:2 (b) index-to-contact ratio CD-1 litters were assessed at day 3 postinoculation and quantified as streptococcal CFU per milligram of homogenized nasal tissue. (c and d) Intranasal GAS tissue burdens from contact and index mice in litters inoculated at 1:1 (c) and 1:2 (d) index-to-contact ratios were likewise assessed at day 11 postinoculation. The geometric mean GAS burdens (red lines) are shown to indicate the mean colonization rate and burden. Litters are indicated by the inocula (CFU) administered, shown on the *x* axis. The limit of detection is indicated by a dotted line (colonization burden, 0.1 CFU/mg). Statistically significant differences in colonization burdens were determined by a Mann-Whitney U test (*, $P < 0.05$; **, $P < 0.01$).

suggesting that the proportion of intranasally infected subjects in a litter influences GAS transmission.

The detection of GAS shed from infant CD-1 mice on days 3 to 9 postinoculation (Fig. 2c to f) and of the intranasal GAS burden at day 11 postinoculation (Fig. 3c and d) demonstrated GAS transmission and persistence in infant mice. In litters inoculated at a 1:1 index-to-contact ratio, GAS transmission and persistence were observed exclusively in litters with index mice administered 10^7 CFU (Fig. 2c and e; Fig. 3a and c; Table 1). The burden of MGAS10870 detected in contact mice from litters with a 1:2 index-to-contact ratio further confirmed that the rate of GAS transmission was directly proportional to the administered inoculum (Fig. 3d; Table 1). The rate of persistence and the intranasal burden of GAS in index mice were also proportional to the inoculum size, with no MGAS10870 being detected in infant mice inoculated with 10^4 CFU (Fig. 3c and d). Additional mouse backgrounds (e.g., C57BL/6 and FVB/NJ) evaluated for GAS strain transmission replicated the inoculum dependence observed in CD-1 mice (Fig. S2). However, C57BL/6 and FVB/NJ infant mice did not demonstrate the dynamic range of shedding and transmission observed with CD-1 mice and therefore were not utilized for further studies.

Altogether, these results show that in the infant mouse model, streptococcal shedding is most apparent in the early acute phase of intranasal colonization. The data indicate that the rate of GAS transmission is influenced by the amount (i.e., shedding titer) and duration of streptococcal output. Persistent shedding resulting in MGAS10870 transmission was associated with higher inocula in index mice (e.g., 10^6 to 10^7 CFU) and a lower index-to-contact ratio (i.e., 1:2). The latter result suggests that the proportion of intranasally colonized subjects in a litter affects the transmission and persistence rates of MGAS10870 in CD-1 infant mice.

TABLE 2 GAS strains used in this study

Strain	*emm* type	Description	Reference[a]
MGAS10870	3	Invasive strain isolated in 2002 in Ontario, Canada[b]	51
emm3$^{\Delta hasA}$	3	Allelic replacement of *hasA* (*SpyM3_1851*) with spectinomycin resistance (*aad9*)	This study
TSPY55	87	Pharyngitis strain isolated in 2013 in Houston, TX[b]	29
emm87(*hasA*^{emm3})	87	Allelic replacement of the native *hasA* promoter and N-terminal region of *hasA* (*SpyM3_1851*) with the equivalent region in the *emm3* strain genome	This study
emm87$^{\Delta covS}$	87	Allelic replacement of *covS* (*SpyM3_0245*) with kanamycin resistance (*aph*)	This study
emm87(*hasA*^{emm3}-Δ*covS*)	87	Allelic replacement of *covS* (*SpyM3_0245*) with kanamycin resistance (*aph*) in the *emm87*(*hasA*^{emm3}) strain	This study

[a]Mutant strains generated for this study are described in the supplemental material.
[b]Harbors the wild-type *covRS* allele.

Restoration of capsule in an acapsular *emm87* strain decreases adherence to human epithelial cells and enhances the ability to grow in human blood. Having established transmission and persistence in the infant mouse intranasal colonization model, we next sought to test the hypothesis that the presence of capsule significantly alters the transmissibility of GAS in a strain-dependent manner. The rationale for our hypothesis is based on multiple lines of evidence that GAS capsule may influence transmission and persistence. The elimination of capsule in capsule-positive strains reduces the ability to colonize in nonhuman primate models of pharyngeal infection (11, 35), suggesting a requirement for acute infection. Conversely, GAS strains cultured from human carriers frequently lack capsule (36–38) secondary to mutations in essential genes (*hasAB*) (28), indicating a selective advantage for persistence in the absence of capsule. Moreover, GAS epidemiological studies show an increase in capsule-negative GAS *emm* types (*emm4*, *emm22*, *emm28*, *emm87*, and *emm89*) (29, 31). We previously showed rapid, fatal, intrafamilial transmission of an *emm87* GAS strain but were unable to assess if the absence of capsule contributed to transmission (39). In addition, the same *emm87* GAS clone contained a frameshift mutation in *covS*, a mutation which in capsule-positive strain backgrounds significantly reduces adherence and transmission while enhancing capsule production (14, 40, 41). Thus, to test our hypothesis, we compared the rates of transmission and persistence of a representative *emm87* GAS strain (TSPY55) with those of the capsule-positive *emm3* strain MGAS10870 as well as isogenic capsule mutants in both serotype backgrounds (Table 2).

Prior to assessing transmission and persistence, we first confirmed predicted phenotypes of parental and capsule mutants in *emm3* and *emm87* backgrounds. Both of the parental *emm3* and *emm87* strains utilized (MGAS10870 and TSPY55, respectively) carry a wild-type functional *covRS* allele. All identified *emm87* strains harbor a frameshift mutation in the *hasA* gene that renders them incapable of producing capsule (29). We restored capsule production to the TSPY55 strain by replacing the native *emm87-hasABC* promoter region with that of MGAS10870, generating the *emm87*(*hasA*^{emm3}) strain (Table 2). The amount of capsule produced by the *emm87*(*hasA*^{emm3}) strain was significantly lower than that of MGAS10870 ($P < 0.001$) (Fig. 4a). The deletion of *covS* by in-frame allelic replacement in *emm87*(*hasA*^{emm3}) resulted in significantly more capsule production than in both its isogenic parent and MGAS10870 ($P < 0.01$) (Fig. 4a). For comparisons in the mouse model, we generated a capsule-negative isogenic mutant of MGAS10870 dubbed *emm3*$^{\Delta hasA}$.

The GAS capsule has previously been shown to interfere with adherence to epithelial cells (23) and enhances GAS resistance to killing by phagocytic immune cells (20, 21). We first examined adherence to cultured primary human tonsillar epithelial cells (HTEpiC) of capsule-negative *emm3* and capsule-positive *emm87* mutants relative to their isogenic parent strains to confirm that the restoration of capsule reduces adherence to human epithelia and vice versa. Both the capsule-positive *emm87*(*hasA*^{emm3}) and *emm87*(*hasA*^{emm3}-Δ*covS*) strains demonstrated decreased adherence to HTEpiC relative to the acapsular *emm87* parent (Fig. 4b). The *emm87*$^{\Delta covS}$ mutant also exhibited less adherence to HTEpiC and was similar to *emm87*(*hasA*^{emm3}). The *emm3*$^{\Delta hasA}$ strain

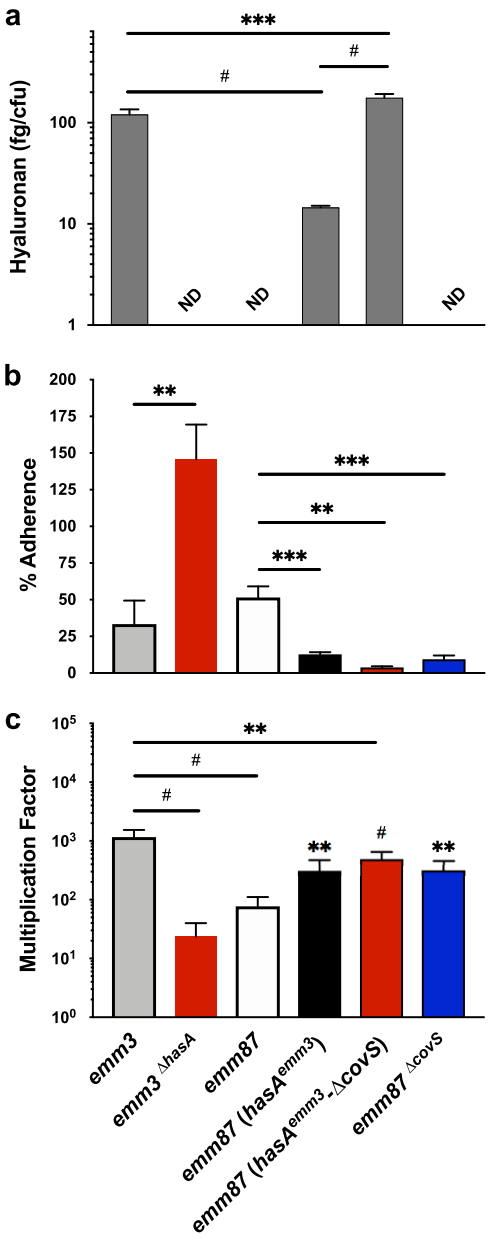

FIG 4 Production of hyaluronic acid capsule reduces GAS adherence to human tonsillar epithelial cells and enhances GAS survival in whole human blood. Hyaluronic acid capsule content (a), adherence to human tonsillar epithelial cells (HTEpiC) (b), and survival in whole human blood (c) were measured in capsule-negative (*emm3*$^{\Delta hasA}$ and *emm87*$^{\Delta covS}$) and capsule-positive [*emm87*(*hasA*^{emm3}) and *emm87*(*hasA*^{emm3}-Δ*covS*)] strains and their respective isogenic parent (*emm87* and *emm3*) strains. The mean hyaluronic acid content was normalized to CFU counts of analyzed GAS cultures and was measured from two biological replicates performed in quadruplicate. Failure to detect capsule is indicated (ND, not detected). The mean percentages of HTEpiC adherence and standard errors of the means (SEM) are shown, calculated from two biological replicates measured in quadruplicate. Adherent *emm87*(*hasA*^{emm3}-Δ*covS*) bacteria were not detected in several replicates. The mean multiplication factors of GAS in whole human blood and SEM are shown, calculated from biological replicates in blood from 3 donors, performed in quadruplicate. Significance was determined by a *t* test (**, $P < 0.01$; ***, $P < 0.001$; #, $P < 0.0001$).

displayed increased adherence to HTEpiC compared to its capsule-positive isogenic parent and showed the highest rate of adherence in the assay (Fig. 4b). We next used the Lancefield bactericidal assay in whole human blood (42) to confirm that the loss of capsule in the *emm3* background reduces resistance to immune clearance and that the production of capsule in the *emm87* background enhances resistance. The rate of

survival of the *emm3*$^{\Delta hasA}$ strain was 50-fold lower than that of the encapsulated strain MGAS10870 ($P < 0.01$) (Fig. 4c). The restoration of capsule production increased the survival of the *emm87* strain (TSPY55) only 3-fold, and the multiplication factor of the *emm87*(*hasA*^{emm3}) strain was similar to that of the *emm87*$^{\Delta covS}$ strain (Fig. 4c). Furthermore, the *emm87*(*hasA*^{emm3}-Δ*covS*) strain showed only a 7-fold increase in the multiplication factor relative to TSPY55, despite producing more capsule than MGAS10870 (Fig. 4a). Thus, the data confirm the predicted effects on adherence and resistance to immune clearance, including subtle but significant *emm* type-dependent differences.

An acapsular *emm87* GAS strain exhibits shedding titers and rates of transmission and persistence distinct from those of an encapsulated *emm3* strain in CD-1 infant mice. The restoration of capsule in the normally capsule-negative *emm87* background predictably led to an increased ability to grow in human blood and decreased adherence to epithelial cells. Thus, we next sought to test the effects of capsule and strain background (capsular versus acapsular) on transmission and persistence using the infant mouse model. To begin, persistence and transmission rates of the capsule-negative *emm87* strain TSPY55 were assessed in mouse litters inoculated at both 1:1 and 1:2 index-to-contact ratios with 10^4 and 10^7 CFU for a baseline comparison with the capsule-positive strain MGAS10870 (Fig. 5). The median titer of TSPY55 detected from mice during the acute shedding period in litters inoculated with 10^7 CFU was significantly lower than that detected from litters given MGAS10870 ($P < 0.05$) (Fig. 5a and b). Likewise, shedding titers of TSPY55 were consistently lower than those of MGAS10870 throughout the monitoring period (Fig. S3a and b). Shedding titers of TSPY55 were directly proportional to the inoculum administered to the litters at an index-to-contact ratio of 1:2 ($P < 0.001$) (Fig. 5b). No shed GAS bacteria were detected from infant mice after the early acute phase in litters inoculated with 10^4 CFU of TSPY55 (data not shown).

TSPY55 was detected in the nasal tissues of several contact mice at both index-to-contact ratios by day 3 postinoculation (Fig. 5c and d; Table 1), notwithstanding that no GAS bacteria shed from these mice were detected at that time (Fig. S3b). The TSPY55 burden in index mice from 1:1 index-to-contact ratio litters was similar to the GAS burden detected in mice inoculated with MGAS10870 (Fig. 5c). However, the median titers of shed TSPY55 and MGAS10870 detected from index mice at the time when nasal tissues were harvested were clearly different (day 3) (Fig. S3a). Although the intranasal burdens of MGAS10870 and TSPY55 differed in index mice of 1:2 index-to-contact ratio litters, no significant differences were detected in colonization rates ($P > 0.05$ by Fisher's exact test) (Fig. 5d).

In direct contrast to MGAS10870, the TSPY55 strain was detected at day 11 in the nasal tissues of contact mice in 1:1 index-to-contact ratio litters administered 10^4 CFU (Fig. 5e; Table 1). TSPY55 also exhibited a higher transmission rate in 1:1 index-to-contact ratio litters administered 10^7 CFU, albeit the difference detected was not statistically significant ($P = 0.13$) (Table 1). TSPY55 persisted in more index mice in 1:1 index-to-contact ratio litters than MGAS10870. The capsule-negative *emm87* strain, which exhibited significantly lower shedding titers than the *emm3* strain at similar inocula, thus persisted and transmitted at a higher frequency at a 1:1 index-to-contact ratio (Fig. 5; Table 1). Conversely, TSPY55 exhibited decreased transmission and persistence rates in 1:2 index-to-contact ratio litters compared to MGAS10870 (Table 1) despite similar GAS tissue burdens being detected in colonized mice between strains (Fig. 5f). Inoculation with the capsule-positive *emm3* strain at a lower index-to-contact ratio (1:2) yielded higher levels of streptococcal shedding and increased persistence and transmission rates, along with the mean GAS burden (Fig. 2; Fig. 3; Table 1). Thus, the index-to-contact ratio differentially affected TSPY55 and MGAS10870 transmission and persistence rates in infant mice.

Production of hyaluronic acid capsule enhances streptococcal shedding of *emm87* and *emm3* GAS strains but influences transmission and persistence in a strain-dependent manner. Inasmuch as all examined *emm87* GAS strains lack capsule through an identical mechanism (frameshift mutation in *hasA*) (29, 43), it is possible

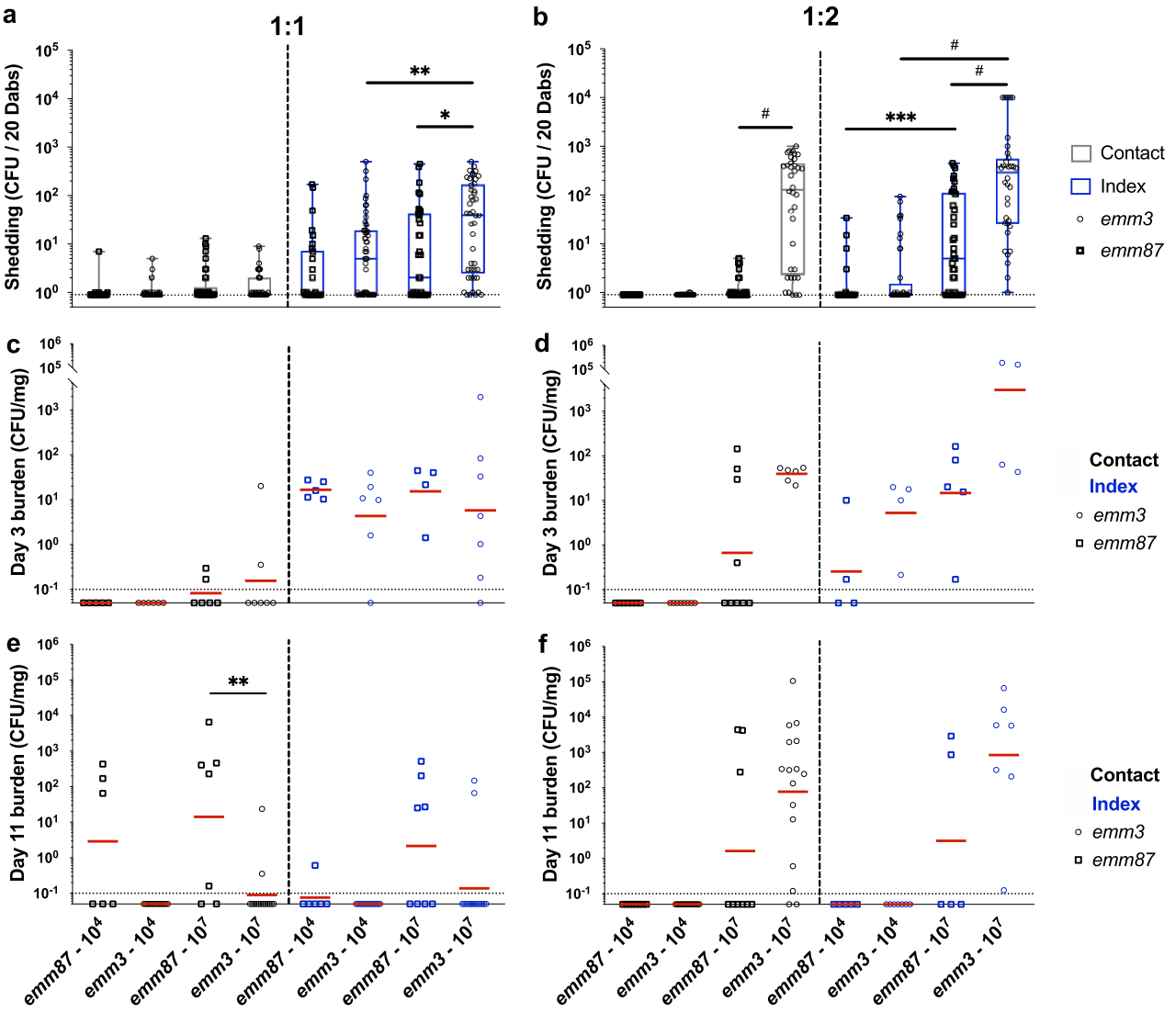

FIG 5 An acapsular *emm87* strain exhibits shedding titers, intranasal persistence, and transmission rates distinct from those of an encapsulated *emm3* strain in CD-1 infant mice. (a and b) Shedding titers of TSPY55 (*emm87*) from index and contact mice in CD-1 litters inoculated at 1:1 (a) and 1:2 (b) index-to-contact ratios were detected and compared to those detected for MGAS10870 (*emm3*) in the acute shedding phase (days 1 to 3 postinoculation). The medians and ranges of detected titers are shown to indicate the median shedding titer and rate. (c and d) Intranasal TSPY55 (*emm87*) GAS tissue burdens in contact and index mice in 1:1 (c) and 1:2 (d) index-to-contact ratio CD-1 litters were assessed at day 3 postinoculation, quantified as streptococcal CFU per milligram of homogenized nasal tissue, and compared to the measured MGAS10870 burden (*emm3*). (e and f) Intranasal GAS tissue burdens from contact and index mice in litters inoculated at 1:1 (e) and 1:2 (f) index-to-contact ratios were likewise assessed at day 11 postinoculation. The *emm3* strain shedding titer and intranasal burden data shown in Fig. 3 are included again here for ease of comparison. The geometric mean intranasal GAS burdens (red lines) are shown to indicate the mean colonization rate and burden. Litters are shown by the strain and inocula (CFU) administered, shown on the *x* axis. The limit of detection is indicated by a dotted line (shedding titer, 1 CFU; colonization burden, 0.1 CFU/mg). Statistically significant differences were determined by a Mann-Whitney U test (*, $P < 0.05$; **, $P < 0.01$; ***, $P < 0.001$; #, $P < 0.0001$).

that *emm87* strains (and perhaps all capsule-negative strains with a similar evolutionary history) have evolved specific mechanisms to aid in transmission and persistence and that restoration of capsule may directly interfere with such mechanisms. Thus, we hypothesized that restoration of capsule in the *emm87* strain background would interfere with transmission and persistence but remain distinct from the *emm3* strain, a strain background that has evolved in the presence of capsule. To test this hypothesis, we examined transmission and persistence rates of parental and isogenic capsule mutants (Table 2) in mouse litters inoculated at a 1:1 index-to-contact ratio with 10^7 CFU (Fig. 6). The shedding titers of the *emm3*$^{\Delta hasA}$ strain detected from all infant mice during the acute shedding phase were significantly lower than those of MGAS10870 ($P < 0.001$) (Fig. 6a and b). Conversely, the shedding titers of the *emm87*(*hasA*^{emm3}) and

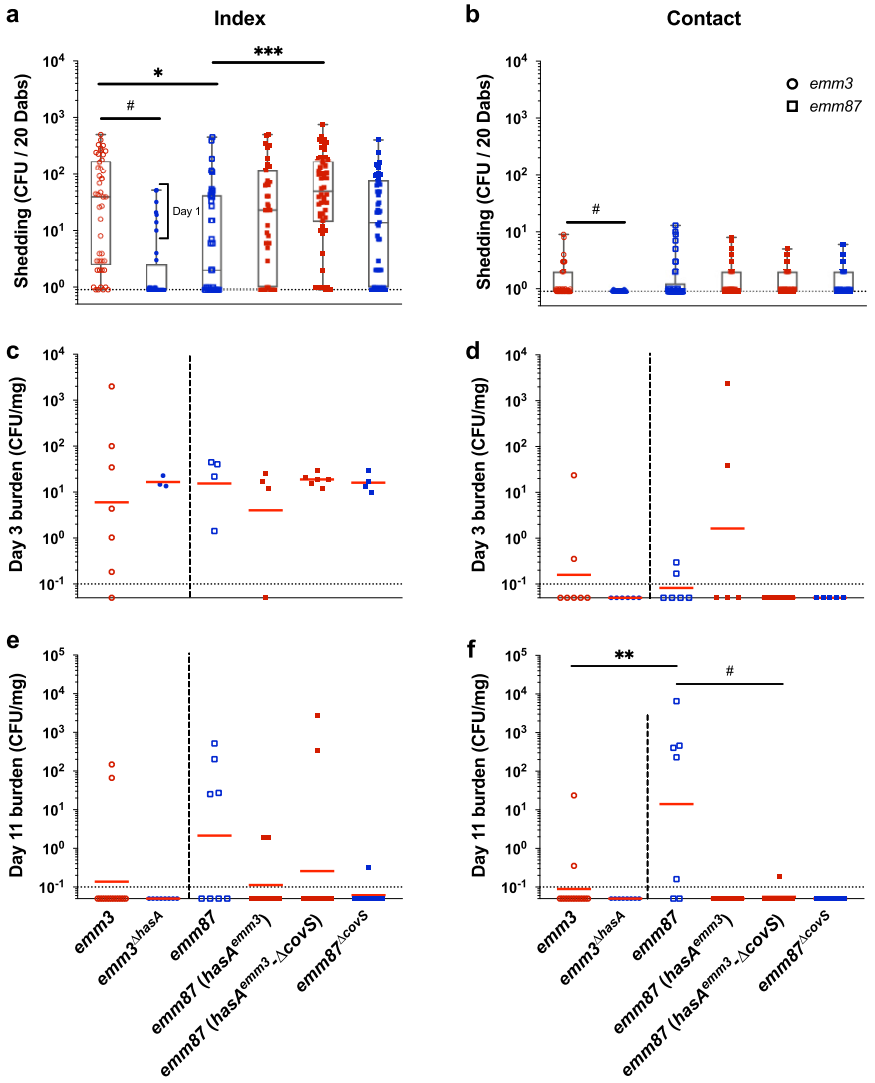

FIG 6 Production of hyaluronic acid capsule enhances shedding of *emm87* and *emm3* GAS strains but influences transmission and persistence in a strain-dependent manner. (a and b) Shedding titers of capsule-negative (*emm3*$^{\Delta hasA}$ and *emm87*$^{\Delta covS}$) and capsule-positive [*emm87*(*hasA*^{emm3}) and *emm87*(*hasA*^{emm3}-Δ*covS*)] mutant GAS strains from index (a) and contact (b) mice in CD-1 litters inoculated at a 1:1 index-to-contact ratio with 10^7 CFU were detected and compared to shedding titers detected for the TSPY55 (*emm87*) and MGAS10870 (*emm3*) isogenic parent strains during the acute shedding phase (days 1 to 3 postinoculation). The medians and ranges of detected titers are shown to indicate the median shedding titer and rate. Litters are indicated by the strain administered, shown on the *x* axis. (c and d) Intranasal GAS tissue burdens of capsule-negative and capsule-positive mutant strains in index (c) and contact (d) mice in CD-1 litters were assessed at day 3 postinoculation, quantified as streptococcal CFU per milligram of homogenized nasal tissue, and compared to the burdens measured in *emm3* and *emm87* strains. (e and f) The intranasal GAS tissue burdens from index (e) and contact (f) mice were likewise assessed at day 11 postinoculation. The geometric mean intranasal GAS burdens (red lines) are shown to indicate the mean colonization rate and burden. The shedding titer and intranasal burden data for the parent *emm3* strain shown in Fig. 3 and the parent *emm87* strain shown in Fig. 5 are included again here for ease of comparison. The limit of detection is indicated by a dotted line (shedding titer, 1 CFU; colonization burden, 0.1 CFU/mg). Significance was determined by a Mann-Whitney U test (*, $P < 0.05$; **, $P < 0.01$; ***, $P < 0.001$; #, $P < 0.0001$).

emm87(*hasA*^{emm3}-Δ*covS*) strains detected from index mice were higher than those of their capsule-negative parent strains throughout the monitoring period (Fig. 6a; Fig. S3c). The median shedding titer of the *emm87*(*hasA*^{emm3}-Δ*covS*) strain during the acute shedding phase was similar to that of the capsule-positive *emm3* strain (Fig. 6a). No shed streptococci were detected beyond the acute shedding phase from mice inoculated with the *emm3*$^{\Delta hasA}$ strain (Fig. S3d). These results indicate that the presence of

capsule enhances GAS shedding in the course of intranasal colonization of CD-1 infant mice.

The nasal tissue burden of GAS detected in index mice selected at day 3 postinoculation indicates that the production of capsule did not alter the intranasal colonization rates of *emm87* and *emm3* strains (Fig. 6c). Paradoxically, the nasal tissue burdens at day 3 in randomly selected contact mice indicate that both the *emm3*$^{\Delta hasA}$ and *emm87*(*hasA*^{emm3}-Δ*covS*) strains failed to transmit during the acute shedding phase (Fig. 6d). This observation was consistent with the low shedding titers of the *emm3*$^{\Delta hasA}$ strain in index mice but was surprising in the case of the *emm87*(*hasA*^{emm3}-Δ*covS*) strain given that restoring capsule production in the *emm87* background enhanced GAS shedding from index mice (Fig. 6a; Fig. S3c). The transmission rate during the acute shedding phase of the *emm87*(*hasA*^{emm3}) strain was similar to that of its isogenic parent.

Examination of nasal tissues at day 11 revealed the absence of *emm3*$^{\Delta hasA}$ streptococci (Fig. 6e and f) and that the loss of capsule failed to enhance *emm3* transmission and persistence (Table 1). In contrast, compared to the *emm3* strain, the acapsular *emm87* strain showed significantly high CFU at day 11 in contact mice ($P < 0.001$) (Fig. 6f), indicating an increased ability to transmit and persist. Capsule-positive *emm87* isogenic mutant strains persisted in fewer index mice than their isogenic parent (Fig. 6e). The lack of *emm87*(*hasA*^{emm3}) and *emm87*(*hasA*^{emm3}-Δ*covS*) streptococci in nasal tissues of contact mice at day 11 postinoculation shows that the restoration of capsule production significantly reduced the transmission of *emm87* GAS ($P < 0.05$) (Table 1; Fig. 6f). Overall, the transmission and persistence data demonstrate that the presence of capsule differentially affects persistence and transmission in a strain-dependent (i.e., capsule-positive versus capsule-negative) manner.

Inactivation of CovRS was shown previously to reduce the shedding and transmission of *emm75* (capsule-positive background) GAS in FVB/NJ adult mice (14). We previously showed rapid, fatal, intrafamilial transmission of an *emm87* GAS strain containing a frameshift mutation in *covS* (39) but were unable to assess if the absence of capsule or the above-mentioned mutation contributed to transmission. To directly address the transmission of *emm87* GAS in the absence of CovRS, we assessed the transmission and persistence phenotypes in the *emm87* strain in the presence (*hasA*^{emm3}-Δ*covS*) and absence (*emm87*$^{\Delta covS}$) of capsule (Table 2). Interestingly, shedding titers of the *emm87*$^{\Delta covS}$ strain were similar to those detected from index mice inoculated with the *emm87*(*hasA*^{emm3}) strain despite differences in capsule production (Fig. 4a; Fig. 6a; Fig. S3c). At day 3 postinoculation, the *emm87*$^{\Delta covS}$ strain colonized index mice at the same rate and at a similar intranasal burden as its isogenic parent (Fig. 6c). The *emm87*$^{\Delta covS}$ strain failed to transmit to contact mice during the acute shedding phase, similar to the *emm87*(*hasA*^{emm3}-Δ*covS*) strain (Fig. 6d), despite the enhanced shedding detected from index mice, which was similar to titers shed from mice administered the *emm87*(*hasA*^{emm3}) strain. The *emm87*$^{\Delta covS}$ strain was not detected in the nasal tissues of contact mice at day 11 postinoculation either, and only one index mouse had any detectable streptococci (Table 1; Fig. 6e and f). Thus, independent of capsule production, the loss of *covS* reduced GAS transmission in the infant mouse model. However, in contrast to the observations of Alam et al. (14), the loss of *covS* increased persistent shedding of capsule-negative *emm87* GAS although not to the extent observed in mice inoculated with the capsule-positive *emm87*(*hasA*^{emm3}-Δ*covS*) strain.

DISCUSSION

Decades of research into the mechanisms of GAS disease have enhanced our understanding of GAS pathogenesis and interactions with the human host. However, despite early investigations of GAS transmission dynamics in humans (7, 8) few studies have directly explored bacterial mechanisms directly contributing to the transmission of GAS, in part due to the lack of feasible models for transmission. Here, we adapted a mouse model designed to investigate transmission in the pneumococcus and con-

firmed the hypothesis that capsule production significantly alters the transmission and persistence of GAS in a strain-dependent manner. The model, in addition to being feasible for most investigators, displayed features consistent with the biology of GAS in humans, including peak shedding during the acute phase of infection (8, 14), a direct correlation between GAS burden and shedding, and detection of colonization extending beyond the acute phase of infection (i.e., persistence). In contrast to previous GAS transmission and persistence models (14), the infant mouse model is amenable to a broader range of GAS inocula for experimentation, in that 10^4 CFU resulted in measurable colonization, transmission, and persistence of GAS among littermates. Using lower inocula than in previous models, our infant mouse model is potentially well suited for comparative studies of *emm* type-specific biology within a host.

The elimination of capsule in capsule-positive strains reduces the ability to persist in nonhuman primate models of pharyngeal infection (11), a phenotype that the *emm3* strain background recapitulated in our infant mouse model. Despite the apparent requirement of capsule for virulence, epidemiological studies show an increase in capsule-negative GAS *emm* types (*emm4*, *emm22*, *emm28*, *emm87*, and *emm89*) (29, 31). Previous investigations of the mechanisms driving the epidemiological success of capsule-negative *emm* types pointed to enhanced expression of cytotoxins such as *nga* and *slo* (44, 45). Zhu et al. proposed that *emm89* strains traded capsule for cytotoxin production as a virulence mechanism that has contributed to capsule-negative serotype emergence (45). Experimentation in our infant mouse model suggests that enhanced transmissibility and persistence may also contribute to the emergence of capsule-negative strains, as at lower inocula, an *emm87* strain transmitted and persisted at higher rates than the capsule-positive *emm3* strain. Our data further indicate that restoring capsule production in a GAS strain that has evolved devoid of capsule (*emm87*), despite expected phenotypic changes in *in vitro* epithelial adherence and *ex vivo* immune resistance, reduced the transmission and persistence rates in the face of increased shedding. The presence of capsule may interfere with molecular mechanisms of the capsule-negative *emm87* strain adapted to transmit and persist in a host in the absence of capsule. Recent work by Turner et al. indicates that *emm87* strains, like the capsule-negative *emm89* strain, also carry a highly active *nga-ifs-slo* promoter (43). Whether enhanced cytotoxin production in the *emm87* background (or other capsule-negative *emm* types) is a molecular mechanism underlying the enhanced transmission and persistence of the capsule-negative serotype can be further investigated using our model.

Our data indicate that *covS* inactivation in the capsule-negative *emm87* background reduced transmission and persistence in the infant mouse and reduced adherence to epithelia yet increased resistance to immune clearance. Investigation of *covS*-dependent virulence phenotypes of the capsule-negative *emm4* serotype determined that *covS* inactivation altered the *emm4* transcriptome in a manner distinct from that observed in capsule-positive strains (46). Consequently, the *emm4* cell surface exhibited increased levels of M protein, fibronectin-binding proteins, and pili, which enhanced *emm4* virulence in a bacteremia model but reduced virulence in a subcutaneous infection model. The altered surface protein expression resulting from *covS* inactivation likely perturbed the interaction of *emm4* GAS with host tissues. Thus, it is possible that *covS* inactivation altered the expression patterns of secreted and surface-localized proteins in *emm87*, resulting in the observed changes in adherence to epithelia, growth in blood, transmission, and persistence. However, further investigation is needed to determine the full effect of CovS inactivation in the *emm87* background.

In our model, the ratio of colonized to uncolonized hosts affected the rates of transmission and persistence in a strain-dependent manner. Contrary to expectation, the transmission of encapsulated *emm3* GAS was favored by a lower density (i.e., 1:2 index-to-contact ratio) of colonized individuals. However, infected host density is not the sole determinant of GAS transmission. Strain-specific differences in capsule production and shedding titers were major contributors to the levels of GAS exposure and transmission. In addition, combined with recently published literature on the role of

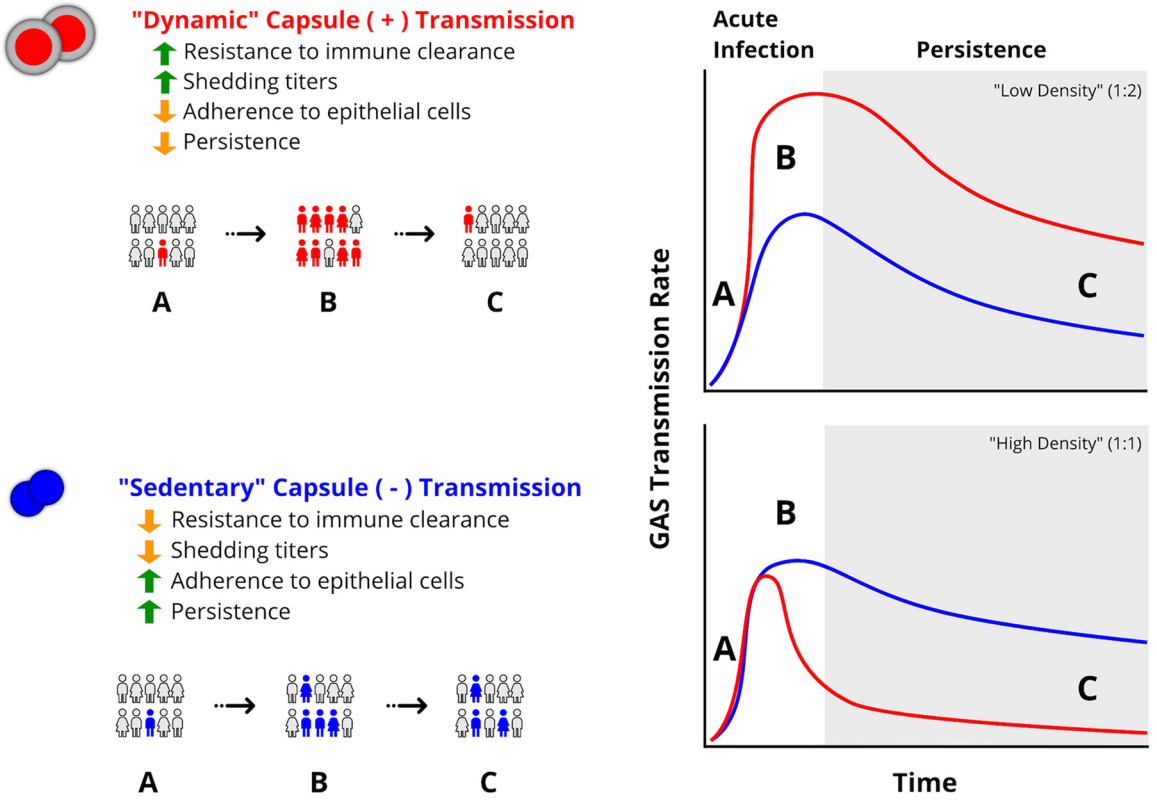

FIG 7 "Dynamic" versus "sedentary" transmission strategies of GAS strains differing in capsule production. Dynamic capsule-positive GAS strains (red) have evolved to transmit in large numbers to naive hosts in a short period of time (B) rather than persisting in the nasopharynx of the colonized host (C). Sedentary capsule-negative GAS strains (blue) transmit at lower titers over a longer period of time (B) and are more likely to persist in contact hosts (C). Differences in GAS transmission burdens observed at a low density of infected individuals (e.g., 1:2) (top right) and a high density of infected individuals (e.g., 1:1) (bottom right) are shown. Each transmission strategy involves contrasting phenotypes of enhanced (green arrows) or reduced (orange arrows) resistance to immune clearance, adherence to epithelia, shedding titers, and colonization persistence.

host inflammatory immune responses in pneumococcal transmission dynamics (47), our data suggest the involvement of host immune responses in the transmission dynamics of GAS. The combination of the type and number of infectious GAS organisms and the resultant host inflammatory response are likely to influence the susceptibility of infant mice to GAS transmission. Thus, it is possible that high-density exposure (1:1 index-to-contact ratio) to *emm3* GAS induced a stronger host inflammatory response, leading to more rapid clearance and reduced detectable GAS transmission and persistence. In contrast to the *emm3* strain, transmission of the capsule-negative *emm87* GAS strain benefited from a higher density of colonized hosts, which is likely the result of lower shedding titers and a less robust inflammatory response, allowing the *emm87* strain to transmit through its enhanced ability to adhere and persist. Future studies are needed to assess the role of host inflammation in the infant mouse model of GAS transmission.

Our data suggest that titers of GAS shed and transmission rates differ between serotypes despite similar bacterial burdens. A combination of the strain-specific GAS shedding titer and the proportion of shedding hosts affects the level of exposure to GAS that results in the effective transmission and persistence of a strain. We propose a model, based on our data, in which capsule production has driven the selection of contrasting infectious strategies among GAS strains, which we define as "dynamic" versus "sedentary" transmission (Fig. 7). Dynamic transmitters (e.g., the *emm3* strain) have evolved to induce high shedding titers and tolerate inflammation through abundant capsule production. Thus, they readily transmit to naive hosts in a short period of time rather than persisting in the nasopharynx of the colonized host. Our

infant mouse model indicated that dynamic transmission is enhanced by low index-to-contact ratios, at which capsule-positive GAS potentially can develop a higher transmission rate through the increased probability of encounters between infected and uninfected subjects (Fig. 7). In contrast, sedentary GAS strains (e.g., the *emm87* strain) have adapted to adhere rather than be shed from colonized host tissue, evolving alternative strategies (e.g., toxin production or expression of cell surface proteins) to subvert host immunity in the absence of capsule (30, 31, 45, 46). Such strains would be more likely to persist in colonized hosts, transmitting over longer periods of time and at a lower rate (Fig. 7). Sedentary transmission is more likely to result in and benefit from higher index-to-contact ratios (e.g., a 1:1 ratio in our studies) due to increased persistence and the dependence on more frequent encounters with infected individuals to increase transmission. In the pneumococcus, an acute inflammatory immune response in nasal tissues is required for robust shedding from colonized infant mice (47), and others have shown that GAS capsule (hyaluronan fragments) may positively or negatively influence inflammatory responses (48, 49). Pneumococci and GAS colonize different niches in the human upper respiratory tract and express distinct virulence factors to resist host immunity, potentially contributing to distinct differences in transmission dynamics. Thus, additional studies are needed to examine the role of the host inflammatory response following infection and its influence on GAS transmission and persistence. The infant mouse model will facilitate such studies and enhance our understanding of host and pathogen mechanisms critical for the emergence and spread of bacterial pathogens.

MATERIALS AND METHODS

Bacterial strains and culture conditions. The strains used in this study are listed in Table 2. GAS strains were grown in Todd-Hewitt broth containing 0.2% (wt/vol) yeast extract (THY broth; Difco Laboratories), on THY agar, on Trypticase soy agar containing 5% sheep blood agar (SBA; Becton, Dickinson), or on Strep Selective II agar (SSIIA; Remel), as indicated. For all *in vitro* assays, cultures were grown overnight in THY broth at 37°C with 5% CO_2 and used to inoculate fresh, prewarmed THY broth for growth to the culture density required. For allelic replacement in mutant strains containing antibiotic resistance cassettes, growth media were supplemented with the corresponding antibiotic (kanamycin or spectinomycin at 150 μg/ml).

GAS colonization, shedding, and transmission in infant mice. GAS intranasal colonization of infant mice and monitoring of GAS persistence and transmission were modeled after the protocol reported previously by Zafar et al. (17), with modifications, and approved by the UT-Health Animal Welfare Committee (AWC). Six- to eight-week-old male and female CD-1 IGS mice (strain code 022; Charles River Laboratories) were bred and maintained in the Center for Laboratory Animal Medicine and Care (CLAMC) facility at UT. The pups were delivered in the CLAMC facility and maintained with their dam for the course of the experiment. Index pups were identified by toe clipping 24 h prior to inoculation. Four-day-old pups were inoculated intranasally without anesthesia with the indicated GAS inocula suspended in 2 μl of sterile PBS. Specifically, the bacterial suspension was placed on the nares with a pipette tip, and the pup was allowed to inhale the inoculum, at which point the pup was returned to its dam. Pups were monitored throughout the course of the experiments (i.e., weight and signs of illness) and appeared healthy and gained weight at a rate similar to that of uninfected animals.

To quantify shedding titers of GAS, the nasal secretions of experimental pups were cultured by gently dabbing the pup snout (20 dabs/mouse) onto SSIIA. The sample was then evenly spread across the agar using a sterile inoculation loop and incubated overnight at 37°C with 5% CO_2. SSIIA contains colistin and oxolinic acid according to the manufacturer's specifications to minimize the growth of contaminants. Beta-hemolytic colonies identified on SSIIA were confirmed to be GAS using a Prolex streptococcal grouping latex kit (catalog number PL.030; Pro-Lab Diagnostics). The limit of detection of shedding titers was 1 CFU/20 dabs. To quantify the nasal GAS burden, at the age of 7 or 14 days (day 3 or 11 postinoculation), infant mice were euthanized by CO_2 asphyxiation followed by cervical dislocation. The nasal cavity was then dissected as described previously (14), weighed, and homogenized in 3 ml of sterile PBS using a TH-01 tissue homogenizer (soft-tissue Omni Tip; Omni International). Tenfold serial dilutions of nasal tissue homogenates were plated onto SSIIA and incubated as indicated above. The limit of detection for nasal GAS burdens was 0.1 CFU/mg of homogenized tissue. Aside from distinguishing between index and contact pups, pups were not individually identified during both dabbing of the nares and nasal tissue harvesting at day 3 postinoculation to maintain randomization in sampling.

Generation of capsule mutants. The plasmids and primers used in this study are listed in Table S1 in the supplemental material. Experimental details are provided in the supplemental material. Briefly, capsule production was restored in the *emm87* background (TSPY55) by the in-frame replacement of the first 783 nucleotides of the *hasA* (*SpyM3_1851*) coding sequence and its native promoter with the homologous sequence of MGAS10870. Capsule production was abrogated in the *emm3* background using a previously described (28, 50) procedure for the allelic in-frame replacement of the *hasA* gene with

a spectinomycin resistance cassette (*aad9*). The same approach was used for the in-frame replacement of the *covS* gene (*SpyM3_0245*) with a kanamycin resistance cassette (*aph*) in the TSPY55 and *emm87*(*hasA*^{emm3}) strains. Mutants were confirmed using targeted sequencing, and whole-genome sequencing confirmed the lack of spurious mutations.

Capsule assay. Capsular hyaluronic acid (HA) levels in tested GAS strains were measured using an HA quantitative test kit (catalog number 029-001; Corgenix) according to the manufacturer's specifications. Samples used to quantify hyaluronic acid were obtained from a 10-ml late-exponential-phase broth culture (THY broth at an optical density at 600 nm [OD_{600}] of 0.6 to 0.8) as previously described (23). Culture serial dilutions were plated onto SBA to quantify CFU for normalization.

Cultured human tonsil epithelial cell adherence assays. Assays of adherence to cultured human epithelial cells were carried out as previously described (28), with modifications. Briefly, approximately 1×10^6 CFU of GAS (multiplicity of infection of ~10) grown to mid-exponential phase (THY broth at an OD_{600} of 0.4) was added to 4 technical replicate wells previously seeded with human tonsil epithelial cells (HTEpiC) cultured according to the supplier's specifications (catalog number 2560; ScienCell Research Laboratories) and incubated for 1 h at 37°C with 5% CO_2. Percent adherence was calculated by dividing the number of CFU recovered on SBA by the number of CFU in the original inoculum.

Survival in human blood. Experiments assessing the ability of GAS to grow in human blood were conducted under a human subject protocol approved by the UT-Health Committee for the Protection of Human Subjects (CPHS). Experiments were carried out as described previously by Lancefield (42). Blood samples from three healthy, nonimmune, adult donors (2 female and 1 male) were used as biological replicates, and assays were performed in quadruplicate (technical replicates).

SUPPLEMENTAL MATERIAL

Supplemental material is available online only.

SUPPLEMENTAL FILE 1, PDF file, 0.5 MB.

ACKNOWLEDGMENTS

This work was supported by grants R01AI125216 and R21AI142126 from the NIH-NIAID (to A.R.F.).

We declare no conflicts of interest.

REFERENCES

1. Barnett TC, Bowen AC, Carapetis JR. 2018. The fall and rise of group A Streptococcus diseases. Epidemiol Infect 147:e4. https://doi.org/10.1017/S0950268818002285.
2. Davies MR, McIntyre L, Mutreja A, Lacey JA, Lees JA, Towers RJ, Duchene S, Smeesters PR, Frost HR, Price DJ, Holden MTG, David S, Giffard PM, Worthing KA, Seale AC, Berkley JA, Harris SR, Rivera-Hernandez T, Berking O, Cork AJ, Torres R, Lithgow T, Strugnell RA, Bergmann R, Nitsche-Schmitz P, Chhatwal GS, Bentley SD, Fraser JD, Moreland NJ, Carapetis JR, Steer AC, Parkhill J, Saul A, Williamson DA, Currie BJ, Tong SYC, Dougan G, Walker MJ. 2019. Atlas of group A streptococcal vaccine candidates compiled using large-scale comparative genomics. Nat Genet 51:1035–1043. https://doi.org/10.1038/s41588-019-0417-8.
3. Wang H, Qin Z, Li M. 2019. Recent advances in pathogenic Streptococcus vaccine development. Curr Issues Mol Biol 32:645–700. https://doi.org/10.21775/cimb.032.645.
4. Casadevall A, Pirofski L. 2000. Host-pathogen interactions: basic concepts of microbial commensalism, colonization, infection, and disease. Infect Immun 68:6511–6518. https://doi.org/10.1128/iai.68.12.6511-6518.2000.
5. Martin JM, Green M, Barbadora KA, Wald ER. 2004. Group A streptococci among school-aged children: clinical characteristics and the carrier state. Pediatrics 114:1212–1219. https://doi.org/10.1542/peds.2004-0133.
6. Efstratiou A, Lamagni T. 2016. Epidemiology of Streptococcus pyogenes, p 621–627. *In* Ferretti JJ, Stevens DL, Fischetti VA (ed), Streptococcus pyogenes: basic biology to clinical manifestations. University of Oklahoma Health Sciences Center, Oklahoma City, OK.
7. Hamburger M, Jr, Green MJ, Hamburger VG. 1945. The problem of the "dangerous carrier" of hemolytic streptococci. I. Number of hemolytic streptococci expelled by carriers with positive and negative nose cultures. J Infect Dis 77:68–81. https://doi.org/10.1093/infdis/77.1.68.
8. Hamburger M, Jr, Green MJ, Hamburger VG. 1945. The problem of the dangerous carrier of hemolytic streptococci; spread of infection by individuals with strongly positive nose cultures who expelled large numbers of hemolytic streptococci. J Infect Dis 77:96–108. https://doi.org/10.1093/infdis/77.2.96.
9. Hysmith ND, Kaplan EL, Cleary PP, Johnson DR, Penfound TA, Dale JB. 2017. Prospective longitudinal analysis of immune responses in pediatric subjects after pharyngeal acquisition of group A streptococci. J Pediatric Infect Dis Soc 6:187–196. https://doi.org/10.1093/jpids/piw070.
10. Johnson DR, Kurlan R, Leckman J, Kaplan EL. 2010. The human immune response to streptococcal extracellular antigens: clinical, diagnostic, and potential pathogenetic implications. Clin Infect Dis 50:481–490. https://doi.org/10.1086/650167.
11. Ashbaugh CD, Moser TJ, Shearer MH, White GL, Kennedy RC, Wessels MR. 2000. Bacterial determinants of persistent throat colonization and the associated immune response in a primate model of human group A streptococcal pharyngeal infection. Cell Microbiol 2:283–292. https://doi.org/10.1046/j.1462-5822.2000.00050.x.
12. Wang X, Fan X, Bi S, Li N, Wang B. 2017. Toll-like receptors 2 and 4-mediated reciprocal Th17 and antibody responses to group A Streptococcus infection. J Infect Dis 215:644–652. https://doi.org/10.1093/infdis/jiw598.
13. Mortensen R, Christensen D, Hansen LB, Christensen JP, Andersen P, Dietrich J. 2017. Local Th17/IgA immunity correlate with protection against intranasal infection with Streptococcus pyogenes. PLoS One 12:e0175707. https://doi.org/10.1371/journal.pone.0175707.
14. Alam FM, Turner CE, Smith K, Wiles S, Sriskandan S. 2013. Inactivation of the CovR/S virulence regulator impairs infection in an improved murine model of Streptococcus pyogenes naso-pharyngeal infection. PLoS One 8:e61655. https://doi.org/10.1371/journal.pone.0061655.
15. Fittipaldi N, Beres SB, Olsen RJ, Kapur V, Shea PR, Watkins ME, Cantu CC, Laucirica DR, Jenkins L, Flores AR, Lovgren M, Ardanuy C, Linares J, Low DE, Tyrrell GJ, Musser JM. 2012. Full-genome dissection of an epidemic of severe invasive disease caused by a hypervirulent, recently emerged clone of group A Streptococcus. Am J Pathol 180:1522–1534. https://doi.org/10.1016/j.ajpath.2011.12.037.
16. Virtaneva K, Graham MR, Porcella SF, Hoe NP, Su H, Graviss EA, Gardner TJ, Allison JE, Lemon WJ, Bailey JR, Parnell MJ, Musser JM. 2003. Group A Streptococcus gene expression in humans and cynomolgus macaques with acute pharyngitis. Infect Immun 71:2199–2207. https://doi.org/10.1128/iai.71.4.2199-2207.2003.
17. Zafar MA, Kono M, Wang Y, Zangari T, Weiser JN. 2016. Infant mouse

model for the study of shedding and transmission during Streptococcus pneumoniae monoinfection. Infect Immun 84:2714–2722. https://doi.org/10.1128/IAI.00416-16.
18. Zafar MA, Hamaguchi S, Zangari T, Cammer M, Weiser JN. 2017. Capsule type and amount affect shedding and transmission of Streptococcus pneumoniae. mBio 8:e00989-17. https://doi.org/10.1128/mBio.00989-17.
19. Wessels MR, Bronze MS. 1994. Critical role of the group A streptococcal capsule in pharyngeal colonization and infection in mice. Proc Natl Acad Sci U S A 91:12238–12242. https://doi.org/10.1073/pnas.91.25.12238.
20. Dale JB, Washburn RG, Marques MB, Wessels MR. 1996. Hyaluronate capsule and surface M protein in resistance to opsonization of group A streptococci. Infect Immun 64:1495–1501. https://doi.org/10.1128/IAI.64.5.1495-1501.1996.
21. Moses AE, Wessels MR, Zalcman K, Alberti S, Natanson-Yaron S, Menes T, Hanski E. 1997. Relative contributions of hyaluronic acid capsule and M protein to virulence in a mucoid strain of the group A Streptococcus. Infect Immun 65:64–71. https://doi.org/10.1128/IAI.65.1.64-71.1997.
22. Husmann LK, Yung DL, Hollingshead SK, Scott JR. 1997. Role of putative virulence factors of Streptococcus pyogenes in mouse models of long-term throat colonization and pneumonia. Infect Immun 65:1422–1430. https://doi.org/10.1128/IAI.65.4.1422-1430.1997.
23. Schrager HM, Rheinwald JG, Wessels MR. 1996. Hyaluronic acid capsule and the role of streptococcal entry into keratinocytes in invasive skin infection. J Clin Invest 98:1954–1958. https://doi.org/10.1172/JCI118998.
24. Hagman MM, Dale JB, Stevens DL. 1999. Comparison of adherence to and penetration of a human laryngeal epithelial cell line by group A streptococci of various M protein types. FEMS Immunol Med Microbiol 23:195–204. https://doi.org/10.1016/S0928-8244(98)00136-9.
25. Darmstadt GL, Mentele L, Podbielski A, Rubens CE. 2000. Role of group A streptococcal virulence factors in adherence to keratinocytes. Infect Immun 68:1215–1221. https://doi.org/10.1128/iai.68.3.1215-1221.2000.
26. Sela S, Neeman R, Keller N, Barzilai A. 2000. Relationship between asymptomatic carriage of Streptococcus pyogenes and the ability of the strains to adhere to and be internalised by cultured epithelial cells. J Med Microbiol 49:499–502. https://doi.org/10.1099/0022-1317-49-6-499.
27. Shea PR, Beres SB, Flores AR, Ewbank AL, Gonzalez-Lugo JH, Martagon-Rosado AJ, Martinez-Gutierrez JC, Rehman HA, Serrano-Gonzalez M, Fittipaldi N, Ayers SD, Webb P, Willey BM, Low DE, Musser JM. 2011. Distinct signatures of diversifying selection revealed by genome analysis of respiratory tract and invasive bacterial populations. Proc Natl Acad Sci U S A 108:5039–5044. https://doi.org/10.1073/pnas.1016282108.
28. Flores AR, Jewell BE, Olsen RJ, Shelburne SA, III, Fittipaldi N, Beres SB, Musser JM. 2014. Asymptomatic carriage of group A streptococcus is associated with elimination of capsule production. Infect Immun 82:3958–3967. https://doi.org/10.1128/IAI.01788-14.
29. Flores AR, Chase McNeil J, Shah B, Van Beneden C, Shelburne SA, III. 2019. Capsule-negative emm types are an increasing cause of pediatric group A streptococcal infections at a large pediatric hospital in Texas. J Pediatric Infect Dis Soc 8:244–250. https://doi.org/10.1093/jpids/piy053.
30. Flores AR, Jewell BE, Fittipaldi N, Beres SB, Musser JM. 2012. Human disease isolates of serotype M4 and M22 group A streptococcus lack genes required for hyaluronic acid capsule biosynthesis. mBio 3:e00413-12. https://doi.org/10.1128/mBio.00413-12.
31. Turner CE, Abbott J, Lamagni T, Holden MT, David S, Jones MD, Game L, Efstratiou A, Sriskandan S. 2015. Emergence of a new highly successful acapsular group A Streptococcus clade of genotype emm89 in the United Kingdom. mBio 6:e00622-15. https://doi.org/10.1128/mBio.00622-15.
32. Kachroo P, Eraso JM, Beres SB, Olsen RJ, Zhu L, Nasser W, Bernard PE, Cantu CC, Saavedra MO, Arredondo MJ, Strope B, Do H, Kumaraswami M, Vuopio J, Grondahl-Yli-Hannuksela K, Kristinsson KG, Gottfredsson M, Pesonen M, Pensar J, Davenport ER, Clark AG, Corander J, Caugant DA, Gaini S, Magnussen MD, Kubiak SL, Nguyen HAT, Long SW, Porter AR, DeLeo FR, Musser JM. 2019. Integrated analysis of population genomics, transcriptomics and virulence provides novel insights into Streptococcus pyogenes pathogenesis. Nat Genet 51:548–559. https://doi.org/10.1038/s41588-018-0343-1.
33. Olsen RJ, Sitkiewicz I, Ayeras AA, Gonulal VE, Cantu C, Beres SB, Green NM, Lei B, Humbird T, Greaver J, Chang E, Ragasa WP, Montgomery CA, Cartwright J, Jr, McGeer A, Low DE, Whitney AR, Cagle PT, Blasdel TL, DeLeo FR, Musser JM. 2010. Decreased necrotizing fasciitis capacity caused by a single nucleotide mutation that alters a multiple gene virulence axis. Proc Natl Acad Sci U S A 107:888–893. https://doi.org/10.1073/pnas.0911811107.
34. Flores AR, Olsen RJ, Cantu C, Pallister KB, Guerra FE, Voyich JM, Musser JM. 2017. Increased pilus production conferred by a naturally occurring mutation alters host-pathogen interaction in favor of carriage in Streptococcus pyogenes. Infect Immun 85:e00949-16. https://doi.org/10.1128/IAI.00949-16.
35. Gryllos I, Cywes C, Shearer MH, Cary M, Kennedy RC, Wessels MR. 2001. Regulation of capsule gene expression by group A Streptococcus during pharyngeal colonization and invasive infection. Mol Microbiol 42:61–74. https://doi.org/10.1046/j.1365-2958.2001.02635.x.
36. Todd EW, Lancefield RC. 1928. Variants of hemolytic streptococci; their relation to type-specific substance, virulence, and toxin. J Exp Med 48:751–767. https://doi.org/10.1084/jem.48.6.751.
37. Ward HK, Lyons C. 1935. Studies on the hemolytic Streptococcus of human origin. I. Observations on the virulent, attenuated, and avirulent variants. J Exp Med 61:515–530. https://doi.org/10.1084/jem.61.4.515.
38. Seastone CV. 1943. The occurrence of mucoid polysaccharide in hemolytic streptococci of human origin. J Exp Med 77:21–28. https://doi.org/10.1084/jem.77.1.21.
39. Flores AR, Luna RA, Runge JK, Shelburne SA, III, Baker CJ. 2017. Cluster of fatal group A streptococcal emm87 infections in a single family: molecular basis for invasion and transmission. J Infect Dis 215:1648–1652. https://doi.org/10.1093/infdis/jix177.
40. Sugareva V, Arlt R, Fiedler T, Riani C, Podbielski A, Kreikemeyer B. 2010. Serotype- and strain-dependent contribution of the sensor kinase CovS of the CovRS two-component system to Streptococcus pyogenes pathogenesis. BMC Microbiol 10:34. https://doi.org/10.1186/1471-2180-10-34.
41. Hollands A, Pence MA, Timmer AM, Osvath SR, Turnbull L, Whitchurch CB, Walker MJ, Nizet V. 2010. Genetic switch to hypervirulence reduces colonization phenotypes of the globally disseminated group A streptococcus M1T1 clone. J Infect Dis 202:11–19. https://doi.org/10.1086/653124.
42. Lancefield RC. 1957. Differentiation of group A streptococci with a common R antigen into three serological types, with special reference to the bactericidal test. J Exp Med 106:525–544. https://doi.org/10.1084/jem.106.4.525.
43. Turner CE, Holden MTG, Blane B, Horner C, Peacock SJ, Sriskandan S. 2019. The emergence of successful Streptococcus pyogenes lineages through convergent pathways of capsule loss and recombination directing high toxin expression. bioRxiv https://doi.org/10.1101/684167.
44. Zhu L, Olsen RJ, Nasser W, Beres SB, Vuopio J, Kristinsson KG, Gottfredsson M, Porter AR, DeLeo FR, Musser JM. 2015. A molecular trigger for intercontinental epidemics of group A Streptococcus. J Clin Invest 125:3545–3559. https://doi.org/10.1172/JCI82478.
45. Zhu L, Olsen RJ, Nasser W, de la Riva Morales I, Musser JM. 2015. Trading capsule for increased cytotoxin production: contribution to virulence of a newly emerged clade of emm89 Streptococcus pyogenes. mBio 6:e01378-15. https://doi.org/10.1128/mBio.01378-15.
46. Galloway-Pena J, DebRoy S, Brumlow C, Li X, Tran TT, Horstmann N, Yao H, Chen K, Wang F, Pan BF, Hawke DH, Thompson EJ, Arias CA, Fowler VG, Jr, Bhatti MM, Kalia A, Flores AR, Shelburne SA. 2018. Hypervirulent group A Streptococcus emergence in an acaspular [*sic*] background is associated with marked remodeling of the bacterial cell surface. PLoS One 13:e0207897. https://doi.org/10.1371/journal.pone.0207897.
47. Zafar MA, Wang Y, Hamaguchi S, Weiser JN. 2017. Host-to-host transmission of Streptococcus pneumoniae is driven by its inflammatory toxin, pneumolysin. Cell Host Microbe 21:73–83. https://doi.org/10.1016/j.chom.2016.12.005.
48. McKee CM, Penno MB, Cowman M, Burdick MD, Strieter RM, Bao C, Noble PW. 1996. Hyaluronan (HA) fragments induce chemokine gene expression in alveolar macrophages. The role of HA size and CD44. J Clin Invest 98:2403–2413. https://doi.org/10.1172/JCI119054.
49. Schommer NN, Muto J, Nizet V, Gallo RL. 2014. Hyaluronan breakdown contributes to immune defense against group A Streptococcus. J Biol Chem 289:26914–26921. https://doi.org/10.1074/jbc.M114.575621.
50. Flores AR, Olsen RJ, Wunsche A, Kumaraswami M, Shelburne SA, III, Carroll RK, Musser JM. 2013. Natural variation in the promoter of the gene encoding the Mga regulator alters host-pathogen interactions in group A Streptococcus carrier strains. Infect Immun 81:4128–4138. https://doi.org/10.1128/IAI.00405-13.
51. Shea PR, Ewbank AL, Gonzalez-Lugo JH, Martagon-Rosado AJ, Martinez-Gutierrez JC, Rehman HA, Serrano-Gonzalez M, Fittipaldi N, Beres SB, Flores AR, Low DE, Willey BM, Musser JM. 2011. Group A Streptococcus emm gene types in pharyngeal isolates, Ontario, Canada, 2002-2010. Emerg Infect Dis 17:2010–2017. https://doi.org/10.3201/eid1711.110159.